

Transmission Loss of a Dissipative Muffler with Perforated Central Pipe

1 Introduction

This example problem demonstrates Coustyx ability to model a dissipative muffler with a perforated central pipe. A dissipative muffler consists of porous material such as fiber glass that helps achieve a much broader band sound attenuation compared to a reactive muffler especially at higher frequencies. Typically the porous material is separated from the flow by perforated pipes to avoid the blowout. Hence to model such a dissipative muffler one needs to accurately model the porous material as well as the perforated pipe, that is in contact with air on one side and porous material on the other side. In this article we would examine various porous material models and perforated interface models. Coustyx simulation results for different models are compared with the experimental measurements presented in [1]. *Multidomain* Coustyx model is used to simulate such problems. A *multidomain* model allows setting up of multiple acoustic domains with different fluid properties which can interact with each other through acoustic interfaces; an acoustic interface relates acoustic variables on either side of interface using transfer matrices. The transmission loss of the muffler is evaluated using the *three-point* method.

2 Problem statement

The dissipative muffler with the perforated central pipe used in this article is adapted from [1] and is shown in Figure 1. The central pipe is assumed to be filled with air at room temperature 19°C with sound speed $c_o = 342651 \text{ mm/s}$ and mean density $\rho_o = 1.204e^{-12} \text{ N s}^2/\text{mm}^4$. The expansion chamber is assumed to be filled with fiber glass of flow resistivity $\sigma = 4896 \text{ mks rayl/m}$. The fiber glass is modeled as an equivalent fluid with complex sound speed \tilde{c} and complex effective density $\tilde{\rho}$ using empirical laws discussed later on. Note that we use $e^{-j\omega t}$ convention throughout this article.

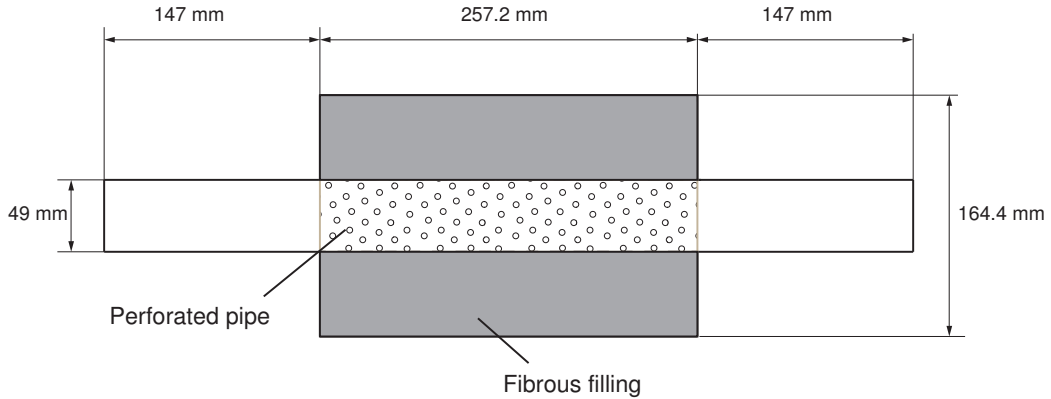


Figure 1: Dissipative muffler.

Figure 2 shows the Coustyx *multidomain* model used. The model is built by defining two separate domains with different fluid medium properties: Domain 1 with air (ρ_o , c_o), and Domain 2 ($\tilde{\rho}$, \tilde{c}) with fiber glass. The two domains interact with each other through perforated interface. The perforated interface is defined through a transfer impedance script and more details are given in next sections. Only a quarter of the muffler is modeled to take advantage of the symmetry in the system and reduce the model size.

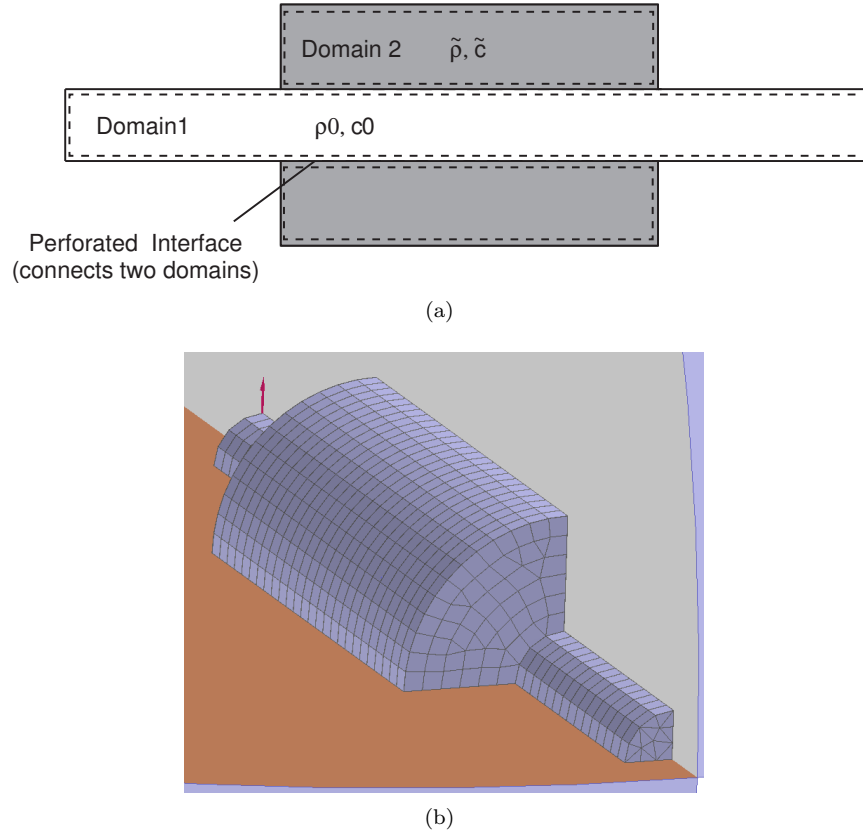


Figure 2: Coustyx multidomain model (a) schematic of two acoustic domains connected by perforated interface, (b) the quarter model used (shown along with two symmetry planes).

3 Porous material modeling

Porous materials are used to absorb (attenuate) sound in many applications. They chiefly consists of pores typically filled with air, and solid materials or *frames* such as fibers, foams, etc., which typically provide viscous and thermal dissipation. For modeling purposes porous materials can be broadly categorized into the following two types:

- **Porous materials with rigid frame.** The solid material or *frame* is assumed to participate in the viscous and thermal dissipation of sound, but not in the wave propagation itself. Most of the fibrous materials such as fiber glass, etc., can be assumed to have rigid frames over a wide frequency range. The porous material in this case can be effectively modeled by replacing it by an equivalent fluid with *bulk properties* such as complex characteristic impedance (\tilde{z}), and complex wave number (\tilde{k}) or by effective complex speed of sound (\tilde{c}) and density ($\tilde{\rho}$). In this article we use empirical laws discussed below to derive these values for the fiber glass filling in the muffler.
- **Porous materials with elastic frame or Poro-elastic materials.** The solid material or *frame* is assumed to be elastic and thus participates in wave propagation in addition to viscous and thermal dissipation of sound. Most types of foams, porous materials sandwiched between elastic structures, etc., come under this category. These materials can't be modeled by the simple equivalent fluid concept. Modeling these materials is beyond the scope of this article.

3.1 Equivalent bulk properties of fiber glass from empirical laws

Empirical laws are commonly used to compute the equivalent fluid properties of porous materials with rigid frame. One such popular law for fibrous materials with porosity close to 1 and flow resistivity σ is given by Delany and Bazley [2],

$$\frac{\tilde{z}}{\rho_o c_o} = \left[1 + 0.057 \left(\frac{\rho_o f}{\sigma} \right)^{-0.754} + j 0.087 \left(\frac{\rho_o f}{\sigma} \right)^{-0.732} \right] \quad (1)$$

$$\frac{\tilde{k}}{(\omega/c_o)} = \left[1 + 0.0978 \left(\frac{\rho_o f}{\sigma} \right)^{-0.7} + j 0.189 \left(\frac{\rho_o f}{\sigma} \right)^{-0.595} \right] \quad (2)$$

where f is the frequency in Hertz. Note that the imaginary value signs are flipped to be consistent with our $e^{-j\omega t}$ convention. Also note that Delany-Bazley law is valid for the range:

$$0.01 < \left(\frac{\rho_o f}{\sigma} \right) < 1.0$$

Another empirical law we are going to use in this article is derived by Lee, et al. [1] from experimental measurements on a fiber glass material of flow resistivity $\sigma = 4896 \text{ mks rayl/m}$ and packing density 100 kg/m^3 . Here again, the imaginary value signs are flipped to be consistent with our $e^{-j\omega t}$ convention.

$$\frac{\tilde{z}}{\rho_o c_o} = \left[1 + 33.20(f)^{-0.7523} + j 28.32(f)^{-0.6512} \right] \quad (3)$$

$$\frac{\tilde{k}}{(\omega/c_o)} = \left[1 + 39.20(f)^{-0.6841} + j 38.39(f)^{-0.6285} \right] \quad (4)$$

The complex sound speed \tilde{c} and effective density $\tilde{\rho}$ are obtained from complex characteristic impedance \tilde{z} and wavenumber \tilde{k} using the following relations:

$$\tilde{z} = \tilde{\rho} \tilde{c} \quad (5)$$

$$\tilde{k} = \frac{\omega}{\tilde{c}} \quad (6)$$

The real and imaginary values of characteristic impedance and wavenumber, from both Lee, et al., and Delany-Bazley empirical laws, for the fiber glass used in this article are compared in Figure 3 and Figure 4.

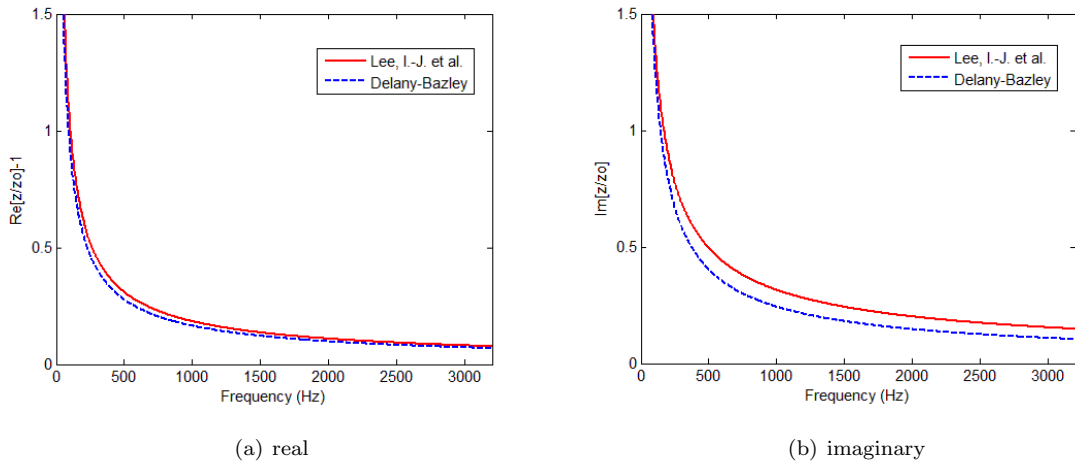


Figure 3: Comparisons of non-dimensional values of characteristic impedance for the fibrous filling used in the muffler from Lee, I.-J. et al. [1] and Delany-Bazley [2] empirical laws.

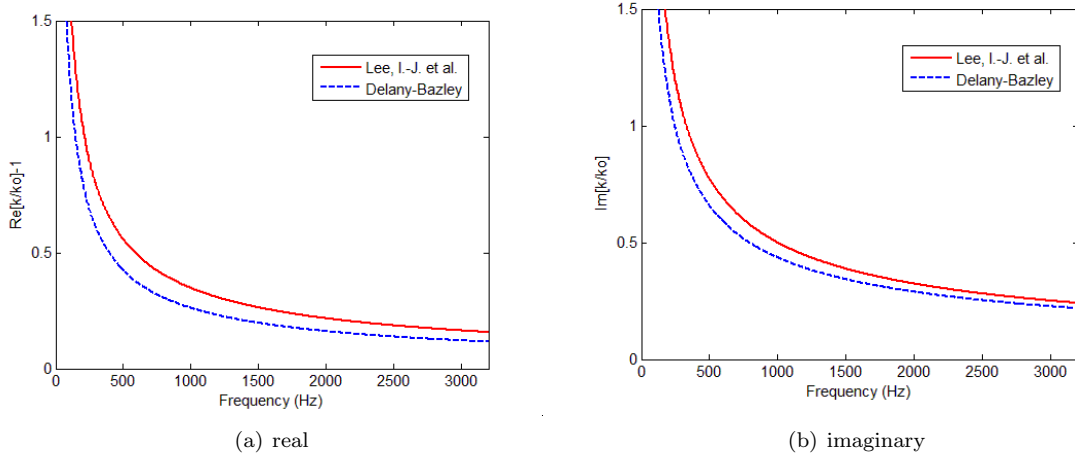


Figure 4: Comparisons of non-dimensional values of wavenumber for the fibrous filling used in the muffler from Lee, I.-J. et al. [1] and Delany-Bazley [2] empirical laws.

4 Perforated interface

A perforated interface defines a special type of transfer relation between acoustic pressures, and acoustic particle normal velocities on both sides of the interface. In the current example, one side of the interface is in Domain 1 (in contact with the air) and the other side of the interface is in Domain 2 (in contact with porous material). If we define the side in contact with air as the negative side of interface ($-$ side) and the side in contact with porous material as the positive side of interface ($+$ side), then the transfer relations for a perforated interface are given by,

$$p^{(+)} - p^{(-)} = -\rho_o c_o \zeta_p v_n^{(-)} \quad (7)$$

$$v_n^{(+)} = v_n^{(-)} \quad (8)$$

where ζ_p is the non-dimensional transfer impedance of the perforated interface; $p^{(+)}$, $p^{(-)}$ and $v_n^{(+)}$, $v_n^{(-)}$ are the acoustic pressures and particle normal velocities on positive and negative sides of the interface. Note that the normal velocities are defined with respect to the interface normal that points from negative side of the interface to the positive side.

The general expression for ζ_p is given by,

$$\zeta_p = \frac{R_h - jX_h}{\phi} \quad (9)$$

$$X_h = k_o (t_w + \alpha d_h) \quad (10)$$

where R_h and X_h are the specific acoustic resistance and reactance of a single hole respectively, ϕ is the porosity defined as the ratio of the open surface area to the total surface area; t_w is the thickness of the pipe, d_h is the hole diameter, α is the total end correction for a hole. Note that we use $e^{-j\omega t}$ convention.

There are many analytical and empirical models available to evaluate R_h and X_h or α of a perforated hole. In [3], Ji gives an analytical model based on works done in references [4, 5, 6] as follows,

$$R_h = \left(1 + \frac{t_w}{d_h}\right) \sqrt{8k_o \mu / z_o} \quad (11)$$

$$\alpha = \frac{4}{\pi^2} \frac{1}{(\xi\eta)^{1/2}} \sum_{m=0}^{\infty} \sum_{n=0}^{\infty} {}_1\varepsilon_{mn} \frac{J_1^2 \left(\pi \sqrt{(m\xi)^2 + (n\eta)^2} \right)}{\left[m^2 \left(\frac{h}{b} \right) + n^2 \left(\frac{b}{h} \right) \right]^{3/2}} \quad (12)$$

where μ is dynamic viscosity of air, $\xi = d_h/b$, $\eta = d_h/h$; b , and h are the distance between adjacent holes in 2-directions; the prime sign on summation means that $m = 0$ and $n = 0$ term is excluded; $\varepsilon_{mn} = 1$ if $m \neq 0$, and $n \neq 0$, and $\varepsilon_{mn} = 0.5$ otherwise; J_1 is the Bessel function of the first kind of order 1. Note that the end correction α expression above is derived in [6] for a circular piston in a rectangular plate.

For air-fibrous contact, Ji [3] modifies Equation 10 to

$$X_h = k_o \left(t_w + \frac{\alpha}{2} \left[1 + \left| \frac{\tilde{k}}{k_o} \right| \left| \frac{\tilde{z}}{z_o} \right| \right] d_h \right) \quad (13)$$

Instead of using analytical models for ζ_p , one can also use empirical relations derived from experimental measurements. A widely used empirical relationship for perforates in contact with air on both sides of the interface (air-air contact) is given by Sullivan and Crocker [7],

$$\zeta_p = \frac{0.006 - jk_o(t_w + 0.75d_h)}{\phi} \quad (14)$$

The above expression was obtained for perforations of porosity $\phi = 4.2\%$. Note that the sign for the imaginary value is flipped to be consistent with our $e^{-j\omega t}$ convention.

In this article, we have used a perforated pipe of following parameters: $\phi = 8.4\%$, $t_w = 0.9$ mm, $d_h = 4.98$ mm, $b = 15.13$, $h = 15.81$. These parameters are similar to the Case C2 in [1], where experiments are conducted to estimate R_h and α in Equation 9 and Equation 10. For air-air contact: $R_h = 0.005318$, $\alpha = 0.4707$; for air-fibrous contact: $R_h = 0.04728$, $\alpha = 0.6206$.

Therefore, the transfer impedance expressions for the current perforated pipe from [1] are given by, air-air contact:

$$\zeta_p = \frac{0.005318 - jk_o(t_w + 0.4707d_h)}{\phi} \quad (15)$$

air-fibrous contact:

$$\zeta_p = \frac{0.04728 - jk_o(t_w + 0.6206d_h)}{\phi} \quad (16)$$

5 Transmission loss

Transmission loss for a muffler can be evaluated by a conventional four-pole method or by an efficient three-point method. In this article we use the three-point method where only a single BEM run is required to evaluate muffler transmission loss.

5.1 Three-point Method

In a three-point method transmission loss is evaluated from the field pressures measured at three points inside the muffler. Among the three points, two of them (points 1, and 2) are located in the inlet pipe and one (point 3) in the outlet pipe (refer to Figure 5). The two field points in the inlet pipe are used to extract the incoming wave pressure (p_i). The field point pressure at point 3 is the same as the transmitted wave pressure (p_t) in the outlet pipe, that is, $p_3 = p_t$. This is due to the specification of anechoic termination at the outlet, which by definition doesn't reflect waves back into the outlet pipe.

Due to the discontinuity in the impedance from the inlet pipe to the expansion chamber of the muffler, a portion of the incoming wave is reflected back to the source. Hence, pressures measured at points 1 and 2 in the inlet pipe are resultant of both the incoming (p_i) and reflected (p_r) waves and are given by [8],

$$p_1 = p_i e^{ikx_1} + p_r e^{-ikx_1} \quad (17)$$

$$p_2 = p_i e^{ikx_2} + p_r e^{-ikx_2} \quad (18)$$

where p_1 , and p_2 are the pressure values; x_1 , and x_2 are the locations of point 1 and point 2 respectively; $i = \sqrt{-1}$. Note that the above equations are little different from the equations specified in [8] due to the adoption of $e^{-i\omega t}$ convention in Coustyx, where ω is the angular frequency.

Solving the above two equations for p_i , we obtain

$$p_i = -\frac{1}{2i \sin k(x_2 - x_1)} [p_1 e^{-ikx_2} - p_2 e^{-ikx_1}] \quad (19)$$

where $\sin k(x_2 - x_1) \neq 0$ or $k(x_2 - x_1) \neq n\pi$, $n = 0, 1, 2, \dots$. Note that the spacing between the points 1 and 2 should be carefully chosen to satisfy this condition at all frequencies.

The transmission loss for a muffler could be evaluated from the incoming (p_i) and the transmitted ($p_t = p_3$) wave pressures [8],

$$TL = 20 \log_{10} \left\{ \frac{|p_i|}{|p_3|} \right\} + 10 \log_{10} \left(\frac{S_i}{S_o} \right) \quad (20)$$

where S_i , and S_o are the inlet and outlet tube areas respectively.

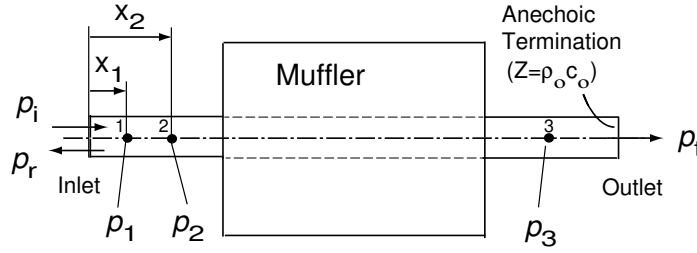


Figure 5: Three-point method [8].

6 Coustyx model setup

A *multidomain* model is used to model the above dissipative muffler in Coustyx. Some of the important model setup steps involved are described below.

- **Generate BE meshes.** Skin the muffler interior to separately generate central pipe and expansion chamber boundary element (BE) meshes. Since only a quarter model is used to take advantage of symmetry, seams need to be specified to avoid skin propagation to the exterior.
- **Specify material properties for air and fiber glass.** The equivalent fluid complex sound speed and effective density for the fiber glass is specified using “scripts”. Equation 3 and Equation 4 are used along with Equation 5 and Equation 6 to define \tilde{c} and $\tilde{\rho}$.
- **Define symmetry planes.**
- **Define interface.** Define a “perforated interface” using *Interfaces* model tree member. Choose *Uniform Perforated* interface type and *Transfer Impedance* as the perforated model type. Define the transfer impedance using “script”.
- **Define domains.** Define two bounded domains: one with air as the acoustic medium and another with fiber glass. Add the central pipe BE mesh to the domain with air, and the expansion chamber BE mesh to the domain with fiber glass. The two domains interact only through the perforated interface. This is achieved by applying interface boundary condition to corresponding elements on both pipe and expansion chamber meshes in the next step. Refer to Figure 6.
- **Boundary conditions.** The following boundary conditions are defined and applied to corresponding elements. Refer to Figure 6.
 - **Inlet:** *Uniform Normal Velocity*, $v_n = -1$.
 - **Outlet:** The muffler outlet is modeled to be *anechoic*. To apply *anechoic* termination, select *Uniform Normal Velocity* BC. Enter a zero value for the structure normal velocity (v_{ns}) through ‘Normal Velocity’ and an ‘Impedance’ value equal to $\rho_o c_o$. That is impedance, $z_o = \rho_o c_o = 412.552e^{-9}$. The anechoic termination BC is applied as, $\frac{p}{v_n - v_{ns}} = z_o$, where p and v_n correspond to the pressure and particle normal velocity on the outlet.

- **Interface:** An *Interface* boundary condition is applied by tagging the BC to “perforated interface” defined above and then identifying the side of the interface it belongs to. An interface has two sides that are arbitrarily assigned as positive and negative sides. We apply the negative side interface BC to elements on the perforated interface in Domain1 (central pipe) and positive side interface BC to elements on the perforated interface in Domain 2 (expansion chamber).
- The rest of the muffler is applied with rigid boundary condition. *Uniform Normal Velocity*, $v_n = 0$

Note that the particle normal velocity v_n in a *multidomain* Coustyx model is always defined with respect to the *Domain Normal*.

- **Analysis script.** Analysis script is created to solve for the field point pressures at the three sensor (microphone) locations as required by the three-point method. Two sensors are placed in near the inlet at distances 30 mm and 60 mm from the inlet face. The incoming wave pressure amplitude in the central pipe is resolved from the results at these sensors using Equation 19. A single sensor is placed near the outlet at a distance of 30 mm from the outlet face to estimate the transmitted wave pressure amplitude in the central pipe. Note that all the three sensors are part of the central pipe, which is Domain 1. Transmission loss is then evaluated using Equation 20 from the sensor results.

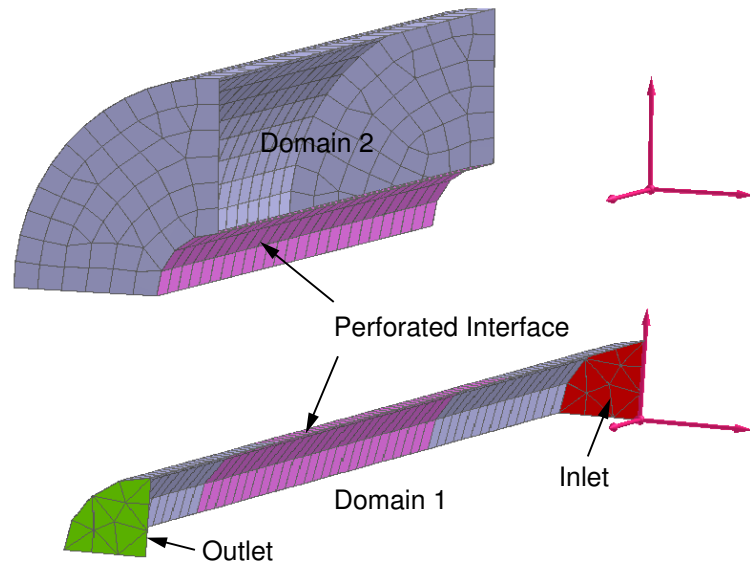


Figure 6: Coustyx (quarter) model shown here with the domains and applied boundary conditions. Note the rest of the model not identified in the figure is applied with rigid boundary condition. Also note that there is no physical separation between elements on perforated interface in domains 1 & 2 (they are separated in the figure only to clarify the boundary conditions).

7 Results and discussion

Several different model cases are examined to understand the effects of porous material models and perforated interface models on the transmission loss predictions. Details of different model cases are described below (summary in Table 7).

- **Model A.** Purely reactive muffler with the perforated pipe. Porous material is removed from the expansion chamber. It is now filled with air just like the central pipe. The perforated interface is modeled using Sullivan and Crocker model as described by Equation 14.

- **Model B.** Purely reactive muffler with the perforated pipe. Porous material is removed from the expansion chamber. It is now filled with air just like the central pipe. The perforated interface is modeled using the analytical transfer impedance expressions (Ji [3]), as described by Equation 11, Equation 12, and Equation 10.
- **Model C.** Purely reactive muffler with the perforated pipe. Porous material is removed from the expansion chamber. It is now filled with air just like the central pipe. The perforated interface is modeled using the empirical relations for transfer impedance computed from experiments by Lee, et al. [1] and as described by Equation 15 air-air contact.
- **Model D.** Dissipative muffler with perforated pipe. The porous material is modeled using Delany-Bazley empirical laws as described by Equation 1 and Equation 2. The perforated interface is modeled using the analytical transfer impedance expressions (Ji [3]) as described by Equation 11, Equation 13, and Equation 12.
- **Model E.** Dissipative muffler with perforated pipe. The porous material is modeled using Delany-Bazley empirical laws as described by Equation 1 and Equation 2. The perforated interface is modeled using the empirical relations for transfer impedance computed from experiments by Lee, et al. [1] and as described by Equation 16 for air-fibrous contact.
- **Model F.** Dissipative muffler with perforated pipe. The porous material is modeled using the empirical expressions derived from experiments by Lee, I.-J. et al. [1] and as described by Equation 3 and Equation 4. The perforated interface is modeled from analytical transfer impedance expressions similar to **Model D**.
- **Model F.** Dissipative muffler with perforated pipe. The porous material is modeled using the empirical expressions derived from experiments by Lee, I.-J. et al. [1] and as described by Equation 3 and Equation 4. The perforated interface is modeled from empirical transfer impedance relation for air-fibrous contact similar to **Model E**.

Table 1: Summary of different model cases examined.

Model	Porous material model	Perforated interface model
A	-	Sullivan-Crocker [7]
B	-	Analytical expression (Ji [3], air-air contact)
C	-	Empirical (Lee, I.-J. et al. [1], air-air contact)
D	Delany-Bazley [2]	Analytical expression (Ji [3], air-fibrous contact)
E	Delany-Bazley [2]	Empirical (Lee, I.-J. et al. [1], air-fibrous contact)
F	Empirical (Lee, I.-J. et al. [1])	Analytical expression (Ji [3], air-fibrous contact)
G	Empirical (Lee, I.-J. et al. [1])	Empirical (Lee, I.-J. et al. [1], air-fibrous contact)

Acoustic analysis is carried out by running an Analysis Sequence in Coustyx model. An Analysis Sequence stores all the parameters required to carry out an analysis, such as frequency of analysis, solution method to be used, etc. The analysis is performed for a frequency range of 60–3200 Hz with a frequency resolution of 20 Hz using the Fast Multipole Method (FMM). Solve the demo model by running the analysis sequence “Run Validation - FMM” to evaluate muffler transmission loss by three-point method. Results are written to the output file “TL.txt”. The output generated by the demo model consists of two columns: first column for analysis frequency in Hertz, and the second column for transmission loss evaluated from Coustyx.

Coustyx *multidomain* model solves for the surface pressures and pressure gradients, which are in turn used to compute field point pressures at the three sensor locations. Transmission loss is then evaluated from Equation 20.

Figure 7 shows the transmission loss comparisons for the reactive muffler with different perforated interface models **Model A-C**. Coustyx results are also compared with experiment measurements extracted from plot in Lee, et al. [1]. It can be seen from the comparisons that different perforated models give different levels of accuracy. **Model A** where the perforated interface is modeled using Sullivan-Crocker model does not give good results. This should be expected as the empirical relation derived by Sullivan-Crocker [7] is for perforates of porosities $\phi = 4.2\%$, but in our case the perforated pipe has porosity $\phi = 8.4\%$.

Figure 8 shows the transmission loss comparisons for the dissipative muffler. Different Coustyx model cases give different levels of accuracy and are compared with the experimental measurements extracted from plots in Lee, et al. [1]. From Figure 7 and Figure 8, we can observe that the porous filling in the dissipative muffler helped achieve a broader band sound attenuation. Also, from the comparisons of different models we can deduce that the transmission loss calculations are very sensitive to the models used to represent the porous material and perforated interface.

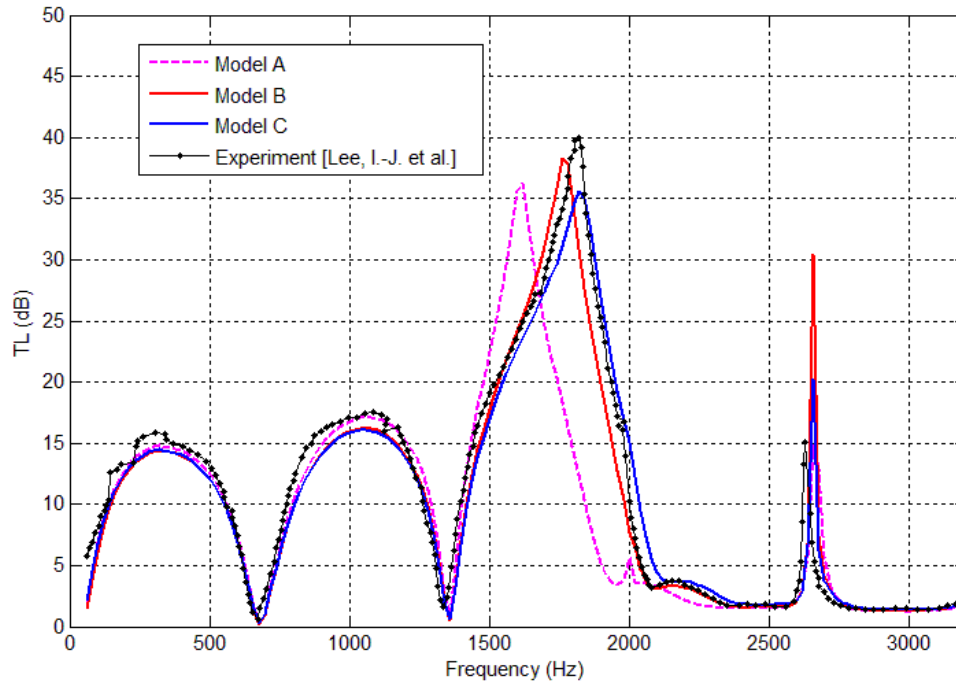


Figure 7: Transmission loss comparisons for the reactive perforated muffler.

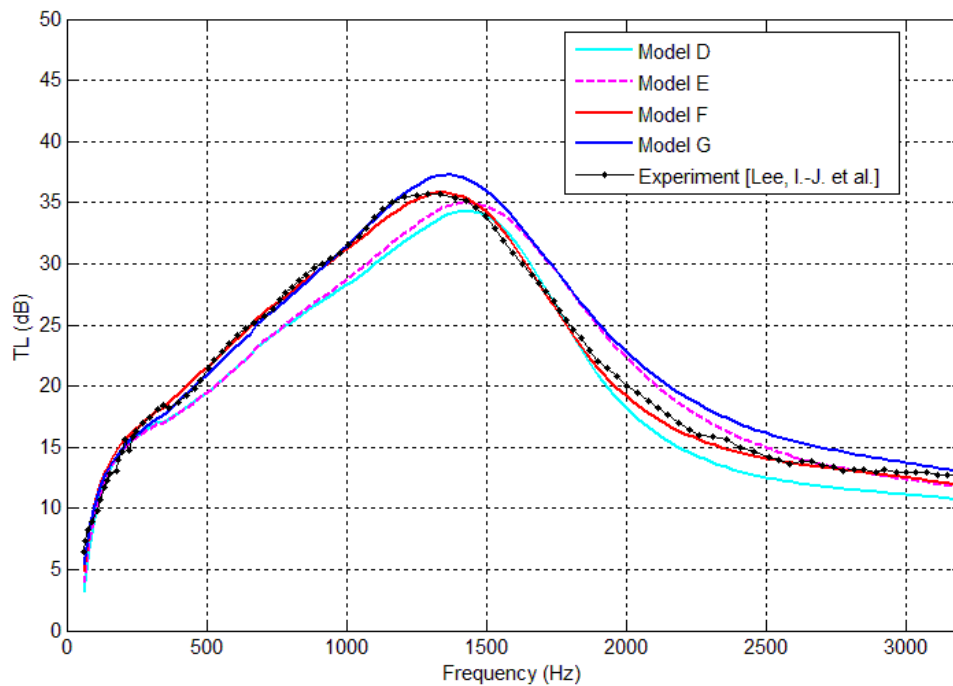


Figure 8: Transmission loss comparisons for the dissipative perforated muffler.

References

- [1] I.-J. Lee, A. Selamet, and N.T. Huff. Acoustic impedance of perforations in contact with fibrous material. *J. Acoust. Soc. Am.*, 119:2785–2797, 2006.
- [2] M.E. Delany and E.N. Bazley. Acoustic properties of fibrous materials. *Applied Acoustics*, pages 105–116, 1970.
- [3] Z. L. Ji. Boundary element acoustic analysis of hybrid expansion chamber silencers with perforated facing. *Engineering Analysis with Boundary Elements*, 34:690–696, 2010.
- [4] T. H. Melling. The acoustic impedance of perforates at medium and high sound pressure levels. *J. Sound Vib.*, 29:1–65, 1973.
- [5] A. B. Bauer. Impedance theory and measurements on porous liners. *J. Aircraft*, 14:720–728, 1977.
- [6] U. Ingard. On the theory and design of acoustic resonators. *J. Acoust. Soc. Am.*, 25:1037–1061, 1953.
- [7] J. W. Sullivan and M. J. Crocker. Analysis of concentric-tube resonators having unpartitioned cavities. *Journal of Acoustic Society of America*, 64:207–215, 1978.
- [8] T.W. Wu and G. C. Wan. Muffler performance studies using a direct mixed-body boundary element method and a three-point method for evaluating transmission loss. *ASME Transaction, Journal of Vibration and Acoustics*, 118:479–484, 1996.